ELSEVIER

Chemical Engineering Journal 71 (1998) 97–109

Chemical Engineering Journal

Simulation of FCC catalyst regeneration in a riser regenerator

D. Bai[a], J-X. Zhu[b,*], Y. Jin[a], Z. Yu[a]

[a] *Department of Chemical Engineering, Tsinghua University, Beijing 100084, China*

[b] *Department of Chemical and Biochemical Engineering, University of Western Ontario, London, Canada N6A 5B9*

Received 5 August 1997; received in revised form 2 June 1998; accepted 16 June 1998

Abstract

A comprehensive one-dimensional model was developed in this work for the simulation of a riser regenerator. The model incorporates the hydrodynamic characteristics of fluidized bed risers and the detailed reaction kinetics of FCC (fluid catalytic cracking) catalyst regeneration and can be used to predict the axial profiles of temperature, oxygen concentration and coke content of the catalyst in the riser. The validity of the present model was confirmed by the experimental data from a pilot demonstration unit. Based on the simulation, effects of solids flow patterns and other parameters including gas velocity, spent and regenerated solids fluxes, temperatures of air and spent catalysts as well as carbon content on the spent catalysts have been systematically examined. The simulation results have provided the necessary information for the optimal design and operation of a FCC riser regenerator unit, presently in operation in China.

Keywords: Fluid catalytic cracking (FCC); Riser regeneration; Fast fluidized bed; FCC regenerator; Computer simulation

1. Introduction

Fluid catalytic cracking (FCC) is one of the key processes in modern petroleum refining [1,2]. While it has evolved significantly in the past 50 years, the technology is still far from perfect. For example, FCC units are now facing many challenges brought about by environmental regulations, product quality demands and economics. One of the major challenges to the refineries comes from the increasing use of resid feed. High residual carbon (e.g. 1.1 wt.% or more) and high metal content (e.g. more than 10 ppm Ni+V) would severely restrict conversion in a typical heat-balanced FCC, leading to rapid catalyst deactivation and extreme regenerator temperature. Therefore, 're-engineering' of FCC regenerators becomes very important and has been the focus of many recent efforts in meeting the needs of using heavier feeds. This is in parallel with the recent advances in FCC reactor technology such as quick-contacting and once-through cracking which may lead to breakthroughs in FCC technology [3–6].

FCC regenerators have experienced many changes over the years. These changes are aimed at higher combustion efficiency, reduced pollutant emissions and reduced catalyst inventory. In general, fluid bed reactor efficiency can be improved by operating at higher gas velocities [7,8]. One particularly successful design is the 'high-efficiency' regenerator [1,2,9]. It uses two-stage combustion. The fast-burning hydrogen-rich components are first combusted at a lower temperature in the first regenerator, which is usually located at the bottom of the unit and operated in the turbulent fluidized bed regime. More than 70 wt.% of the coke and most of the hydrogen are burned at this first stage. The low temperature (maximum 700°C) and incomplete burn-off of carbon effectively limits catalyst deactivation due to steaming generated from hydrogen combustion. From the first stage regenerator, solids are entrained through a riser and an inertial separator into the upper second regenerator, where the slow-burning residual coke is combusted at a high temperature (commonly above 800°C) in a dry environment of excess air. This allows the coke to be burned clean with minimal catalyst hydrothermal deactivation.

To further increase combustion efficiency and reduce catalyst inventory, a riser catalyst regenerator has been proposed (e.g. [10]). The concept is based on the considerable advantages of fluidized risers, including large capacity, higher gas–solids contact efficiency, high heat/mass transfer rates and low solids inventory. This technology carries out the coke combustion in a riser operating in a typical fast fluidization regime. A typical riser regenerator is

*Corresponding author. Tel.: +1-519-661-2131; fax: +1-519-661-3498; e-mail: jzhu@julian.uwo.ca

1385-8947/98/$ – see front matter
PII: S1385-8947(98)00110-7

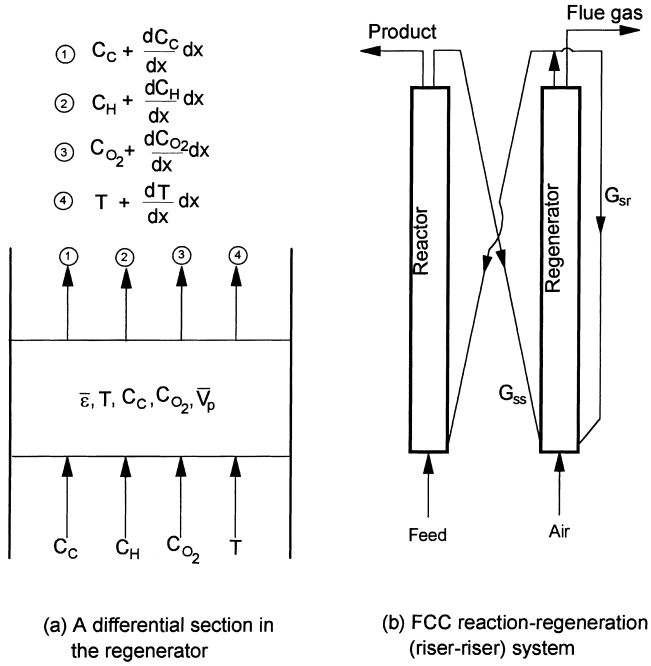

Fig. 1. Schematic diagram of FCC reaction–regeneration system.

schematically illustrated in Fig. 1. Fresh air and spent catalysts are mixed at the riser bottom and move upward along the riser. The catalyst particles are separated from the flue gas in a separator at the riser top. Part of the regenerated catalyst is returned to the base of the riser regenerator to maintain the riser regenerator temperature, and the rest is recirculated to the riser reactor.

Engelhard Corporation [11] developed a circulating fluidized reactor model for the design and development of the ART catalyst riser regenerator. A 10 m diameter commercial ART CFB regenerator is reported to be in operation in Kentucky. They found from the simulation that coke contents of the feed catalyst, gas velocity and coke reactivity significantly affect the regenerator performance, but the effects of catalyst circulation rate, bed diameter and solids mixing appear to be relatively minor. Because of the high coke content (1.3–3.2 wt.%) in the ART process, the existence of a premix zone below the CFB regenerator and, consequently high temperature (under most conditions higher than 670°C in the bed entrance and up to 840°C in the exit), they concluded that coke conversion should be complete within a small vertical distance. However, this is not the case considered here for a FCC catalyst regenerator where regeneration temperature should be strictly controlled under 750°C, since otherwise the catalyst will be over burned and deactivated permanently.

For design and development of FCC catalyst riser regenerators, a one-dimensional model was developed in this work. The model consists of sub-models for hydrodynamics with adjustable solids mixing patterns and the detailed reaction kinetics of catalyst regeneration. The simulation has focused on understanding the regeneration performance under different conditions and searching for the optimal operating conditions. Various factors that might influence the regeneration performance have been examined. Some findings beneficial to the design and operation of FCC catalyst riser regenerator are also reported.

2. Model development

The FCC catalyst riser regeneration model consists of two major parts, the hydrodynamics in the riser and the kinetics of FCC catalyst regeneration. In this work, the gas is treated as plug flow, and the solids are assumed as either plug flow or complete mixing flow. According to the catalyst regeneration characteristics, it is reasonably assumed that the change in the molar flowrate of the gas during the regeneration reaction can be neglected. The specific heat capacity of the catalyst is considered the same as the coke. Since the pressure drop across the riser is low, the pressure in the regenerator is taken as constant. Based on these assumptions and the schematic shown in Fig. 1(a), the reaction model and heat balance equations for solids flow in PF (plug flow) mode and CSTR (complete stirred tank reactor) mode are derived and summarized in Table 1. To solve these equations, one must provide the riser hydrodynamics for the estimation of voidage and its axial distribution, the regeneration reaction kinetics as well as the initial conditions.

2.1. Hydrodynamics

The one-dimensional model developed by Bai et al. [12,13], taking into account the solids acceleration section in the riser entrance, is employed to estimate the voidage and its axial variation along the riser. The model treats the

Table 1
Summary of PF and CSTR model equations

	PF mode	CSTR mode
Coke	$dC_C/dx = -r_C\rho_p(1-\bar{\epsilon})/G_s$	$C_{Cs} - C_{C,out}/G_{ss} = (x_{O_2} - x_{O_{2,out}})12p_0U_{g0}/(1+3\alpha)RT_0$
Hydrogen	$dC_{H_2}/dx = -r_H\rho_p(1-\bar{\epsilon})/G_s$	Complete reaction
Oxygen	$dC_{O_2}/dx = -(r_C/12 + 1/2r_H/4)\rho_p(1-\bar{\epsilon})/U_g$ $dx_{O_2}/dx = -(r_C/12 + 1/2r_H/4)\rho_p(1-\bar{\epsilon})/(U_g p/RT)$	$dC_{O_2}/dx = -1/12\rho_p(1-\bar{\epsilon}_v)/U_g$ $dx_{O_2}/dx = -1/12\rho_p(1-\bar{\epsilon}_v)RT/pU_g$
Heat	$dT/dx = \rho_p(1-\bar{\epsilon})(r_C\Delta H_C + r_H\Delta H_H)/U_{g0}\rho_{g0}c_{pg} + G_s c_{pc}$	$T_g = G_{ss}T_s c_{pc} + G_{sr}c_{pc}T'_g + U_{g0}\rho c_{pg}T_a + \Delta H/G_{ss}c_{pc} + G_{sr}c_{pc} + U_{g0}\rho c_{pg}$

gas and solids as two interpenetrating fluids and assumes that the pressure drop is only due to the gas phase. Then, for one-dimensional steady flow, the continuity equations are

$$\frac{\mathrm{d}(\bar{\epsilon}\rho_g \bar{V}_g)}{\mathrm{d}x} = 0 \tag{1}$$

$$\frac{\mathrm{d}[(1-\bar{\epsilon})\rho_p \bar{V}_p]}{\mathrm{d}x} = 0 \tag{2}$$

and the momentum equations are

$$\frac{\mathrm{d}(\bar{\epsilon}\rho_g \bar{V}_g^2)}{\mathrm{d}x} = -\frac{\mathrm{d}p}{\mathrm{d}x} - F_D - \bar{\epsilon}\rho_g g - F_g \tag{3}$$

$$\frac{\mathrm{d}[(1-\bar{\epsilon})\rho_p \bar{V}_p^2]}{\mathrm{d}x} = F_D - (1-\bar{\epsilon})\rho_p g - F_p \tag{4}$$

$$F_D = \frac{3}{4}\frac{1-\bar{\epsilon}}{d_p} C_D \rho_g (\bar{V}_g - \bar{V}_p)^2 \tag{5}$$

Taking into account the drag reduction due to solids aggregation, the actual drag coefficient can be obtained by [13]

$$\frac{C_D}{C_{DS}} = 1.68\,\bar{\epsilon}^{0.25}\left(\frac{\mathrm{Re_t}}{\mathrm{Re_r}}\right)^{-1.21}\left(\frac{d_p}{D}\right)^{0.11} \tag{6}$$

C_{DS} stands for the standard drag coefficient of a single particle in a uniform flow, and can be calculated by [14]

$$\begin{cases} C_{DS} = \dfrac{24}{\mathrm{Re_r}} + \dfrac{3.6}{\mathrm{Re_r}^{0.313}} & (\mathrm{Re_r} \le 2000) \\ C_{DS} = 0.44 & (\mathrm{Re_r} > 2000) \end{cases} \tag{7}$$

The frictional shear forces of gas and solids against the wall, F_g and F_p, can be expressed by

$$F_g = \frac{2 f_g \rho_g \bar{\epsilon} \bar{V}_g^2}{D} \tag{8}$$

$$F_p = \frac{2 f_p \rho_p (1-\bar{\epsilon}) \bar{V}_p^2}{D} \tag{9}$$

where the gas friction coefficient, f_g, can be estimated by

$$\begin{cases} f_g = \dfrac{16}{\mathrm{Re}} & (\text{when } \mathrm{Re} \le 2000) \\ f_g = \dfrac{0.079}{\mathrm{Re}^{0.313}} & (\text{when } \mathrm{Re} > 2000) \end{cases} \tag{10}$$

and the solids phase friction coefficient, f_p, can be estimated by the following empirical equation originally proposed by Martin and Michaelides [15]

$$f_p = \left[\left(1 + \frac{G_s}{G_g}\right)^{0.3} - 1\right] f_g \tag{11}$$

2.2. Regeneration kinetics

Regeneration of spent catalyst is a very complicated process involving both gas–solids reactions (e.g. carbon burning and hydrogen burning) and gas phase reactions (e.g. CO combustion). A general scheme of the reaction can be expressed by [16]

$$\mathrm{CH_{12\alpha}} + \left(\frac{\beta + 0.5}{\beta + 1} + 3\alpha\right)\mathrm{O_2} \rightarrow \frac{\beta}{\beta+1}\mathrm{CO_2} + \frac{1}{\beta+1}\mathrm{CO} + 6\alpha\mathrm{H_2O} \tag{12}$$

where α is the hydrogen to carbon mass ratio in the coke and β is the molar ratio of CO_2 to CO in the flue gas. In the case of complete combustion regeneration, $\beta = \mathrm{CO_2/CO} = \infty$, the above reaction scheme becomes:

$$\mathrm{CH_{12\alpha}} + (1 + 3\alpha)\mathrm{O_2} \rightarrow \mathrm{CO_2} + 6\alpha\mathrm{H_2O} \tag{13}$$

It has been found that coke ($CH_{12\alpha}$) containing carbon and hydrogen is generally combusted in two different steps, carbon burning and hydrogen burning [17–19]. For carbon burning, the reaction rate is dependent on the catalyst properties but not on the materials from which coke forms. For CRC-1 catalyst, a FCC catalyst widely used in China, the burning rate has been given by Mo et al. [17,18]

$$-\frac{\mathrm{dC_C}}{\mathrm{d}t} = k_C p_{O_2} \mathrm{C_C} \tag{14}$$

where

$$k_C = 1.65 \times 10^8 \exp\left(-\frac{1.612 \times 10^5}{RT}\right) \tag{15}$$

For hydrogen combustion, the combustion rate for the CRC-1 catalyst can be represented by [19]

$$-\frac{\mathrm{dC_H}}{\mathrm{d}t} = k_H p_{O_2} \mathrm{C_H} \tag{16}$$

where

$$\begin{cases} k_H = 2.44 \times 10^8 \exp\left(-\dfrac{1.577 \times 10^5}{RT}\right) & (T < 973\,\mathrm{K}) \\ k_H = 2.44 \times 10^8 \exp\left(-\dfrac{1.577 \times 10^5}{RT}\right)\left[1 - 2.67 \times 10^{30} \exp\left(-\dfrac{7.34 \times 10^4}{RT}\right)\right] & (T > 973\,\mathrm{K}) \end{cases} \tag{17}$$

It is seen from the above equations that the rate of hydrogen combustion is about 2.5 times higher than that of carbon combustion. In the reaction process, the ratio of hydrogen (H) to carbon (C) is

$$\alpha = \alpha_0 \exp[-(k_C - k_H) p_{O_2} t] \tag{18}$$

2.3. Initial conditions

The PF mode shown in Table 1 consists of a set of differential equations that can be solved by numerical Runge–Kutta method. The boundary conditions (at x=0)

Table 2
Comparison of coke combustion intensities between different regenerators

	One-stage regenerator	Two-stage regenerator	High-efficiency tank	Riser regenerator
Coke combustion intensity (kg/t h)	~100	100~300	200~500	>1000

are given by

$$\begin{cases} x &= 0 \\ x_{O_2} &= 0.21 \\ \bar{\epsilon} &= \epsilon_a \\ C_C &= \dfrac{G_{ss}C_{Cs} + G_{sr}C_{C,out}}{G_{ss} + G_{sr}} \\ C_H &= \dfrac{\alpha G_{ss}C_{Cs} + G_{sr}C_{H,out}}{G_{ss} + G_{sr}} \\ T &= \dfrac{G_{ss}c_{pc}T_s + G_{sr}c_{pc}T'_g + U_{g0}\rho_{g0}c_{pg}T_a}{G_{ss}c_{pc} + G_{sr}c_{pc} + U_{g0}\rho_{g0}c_{pg}} \end{cases} \quad (19)$$

Eq. (19) indicates that the contents of carbon and hydrogen as well as temperature in the riser entrance are functions of those at the riser outlet. Therefore, an iteration is performed to solve the problem. The voidage in the bottom of the riser, ϵ_a, is calculated by the empirical correlation of Kwauk et al. [20].

For CSTR flow mode (see Table 1) the boundary condition for the oxygen balance equation is the same as for PF flow mode. In this case, the axial voidage profile predicted by the one-dimensional model is integrated over the riser height to obtain an average bed voidage, $\bar{\epsilon}_v$. This ensures the

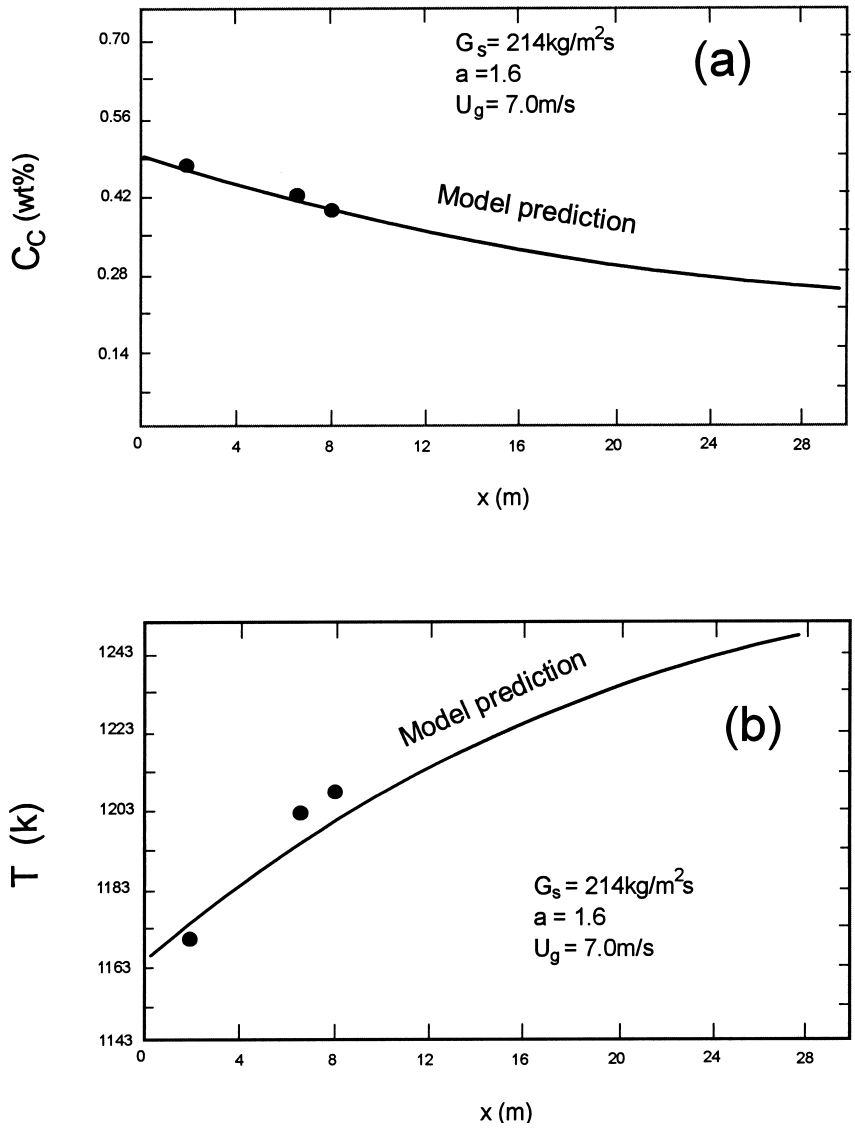

Fig. 2. Comparison between the predicted (solid line) and the measured (solid circle) carbon content and temperature for the Dagang industrial riser regenerator.

same amount of catalyst is included in the reactions in both PF mode and CSTR mode, giving the same comparison base for the two flow modes. Iterations are also needed to solve the equations for the CSTR mode.

3. Simulation results and discussion

Table 2 summarizes the coke combustion intensities for different regenerators [21]. It is seen that the riser regenerator has significant advantage over the others, with considerable larger coke combustion intensity. This benefits from the good contacting between gas and solids as well as the high solids circulation that greatly increases the unit capacity. Clearly, riser regenerators can achieve high combustion efficiency and intensity with lower solids inventory. This will significantly reduce the equipment cost and lead to larger profits.

3.1. Validation of the model predictions

An industrial high-efficiency regenerator with a capacity of 5×10^4 t/a is in operation in a refinery in Dagang on the eastern coast of China. Below the second-stage turbulent fluidized bed regenerator, there is a 8 m long riser, which serves for catalyst premixing as well as regeneration. Samples of catalyst were withdrawn from three locations along the riser, from which the carbon content on the catalyst was analyzed. The temperatures in these locations were also recorded. The superficial gas velocity at the riser entrance is 7 m/s, and the solids circulation rate inside the riser is estimated as 214 kg/m^{2}s from the carbon balance. Based on the work of Bai et al. [22], the flow pattern in the riser corresponding to the above operating condition is expected to be in the transition region from fast fluidization to pneumatic transport, suggesting a gas–solids flow pattern similar to plug flow. A comparison between the predictions by the PF flow model and the industrial data is given in Fig. 2. Without introducing any equipment-adjustable parameters, a good agreement between model predictions and experimental data is obtained. This confirms the validity of the present model.

3.2. Axial profiles of C, H, O_2, T and the influence of solids mixing pattern

With the validation of the present model, computer simulations were carried out with operating conditions typically encountered in a refinery FCC riser regenerator. When catalyst particles are assumed as plug flow, a typical simulation result by the PF model is shown in Fig. 3. It is seen that with the progress of regeneration reaction, the contents of C and H on catalysts and O_2 concentration in fuel gas continuously decrease and the temperature continuously increases along the riser. In the entrance region, the high solids concentration, high C and H contents on the catalyst and high O_2 concentration lead to high reaction rates. Therefore, there are large axial variations in the reactant concentrations and temperature. Up the riser, O_2 is largely consumed. As well, solids concentration becomes low and varies little along the axial position. This results in low reaction rates and relatively small changes in the reactant concentrations and temperature along the riser, suggesting that the regeneration becomes more difficult up the riser.

Fig. 4 shows the simulation results by the CSTR model. Variation of O_2 is similar to that observed in the PF flow model. Since solids are assumed to be completely mixed, the carbon content (C) on the catalyst and the temperature are uniform throughout the riser.

The carbon content on the catalyst at the riser exit, $C_{C,out}$, is plotted against the ratio of regenerated catalyst flowrate to spent catalyst flowrate, $a = G_{sr}/G_{ss}$, in Fig. 5 for gas velocities of 3, 3.5 and 4 m/s. In general, the regeneration performance for the PF model is better than for the CSTR model at higher a. This trend reverses itself at lower a. To explain this phenomenon, the axial profiles of carbon content and temperature for three values of a are illustrated in

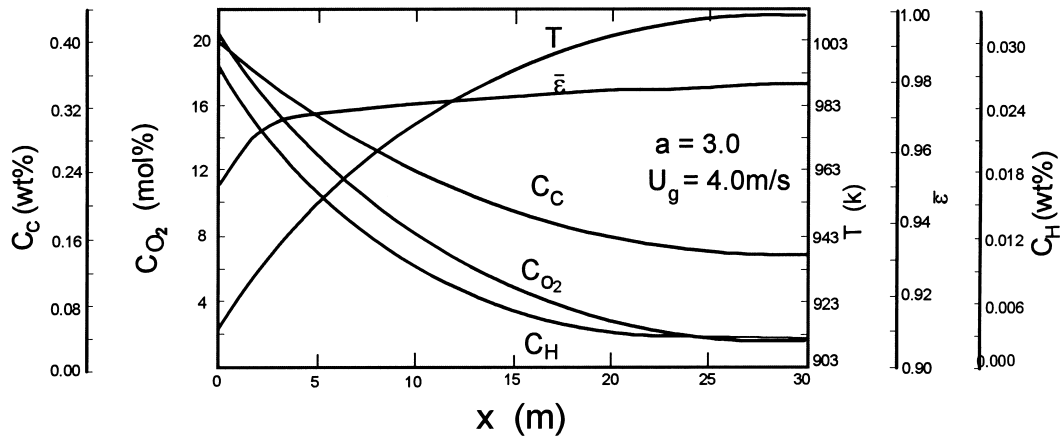

Fig. 3. Axial profiles of C_C, C_H, C_{O_2}, T and $\bar{\varepsilon}$ predicted by the plug flow model for U_{g0}=4 m/s, G_{ss}=40 kg/m^2 s and a=3.0.

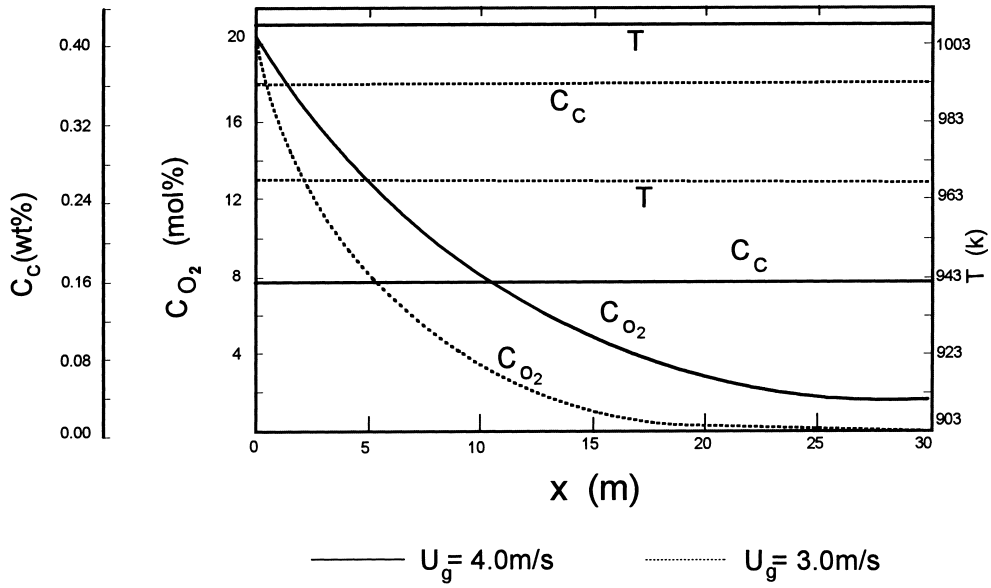

Fig. 4. Axial profiles of C_C, C_{O_2} and T predicted by the CSTR flow model for U_{g0}=3 m/s and 4 m/s, G_{ss}=40 kg/m^2 s and a=3.0.

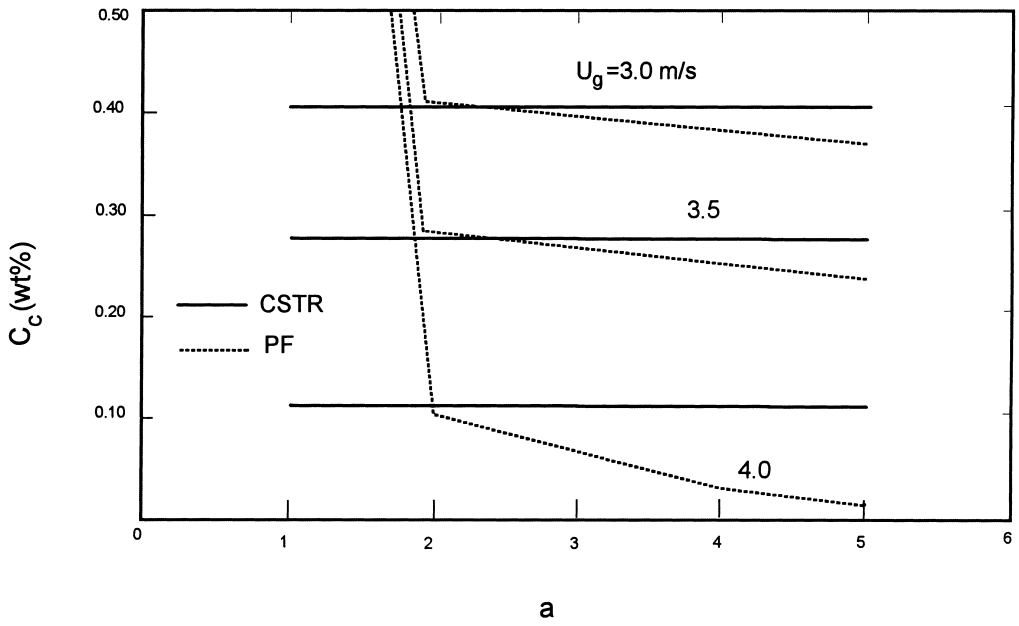

Fig. 5. Carbon contents (C_C) at the riser exit predicted by the PF model (dashed lines) and the CSTR model (solid lines).

Fig. 6. It is seen that when a is small (Fig. 6(a)), though the initial carbon content for the PF mode is higher than for the CSTR mode, the high temperature in the CSTR mode leads to a significant higher reaction rate, so that $C_{C,out}$ (CSTR)<$C_{C,out}$ (PF). As a is increased (Fig. 6(b)), the temperatures for the two flow modes become closer, especially in the entrance region. Further increasing a leads to a considerable increase in temperature for the PF mode (Fig. 6(c)), so that the PF mode gives better regeneration performance than the CSTR mode, i.e. $C_{C,out}$ (CSTR)> $C_{C,out}$ (PF). The above findings imply that to improve the regeneration performance attempts should be made to have the riser regenerator operated close to the CSTR mode when α is small, otherwise, a plug flow would be preferable. In the following sections, discussions on the influencing factors will be mainly based on the simulation results by the PF model.

3.3. Influence of superficial gas velocity

Changing the superficial gas velocity affect the regeneration performance in the following three manners: (1) it leads to the variation of oxygen concentration; (2) it changes the reaction temperature since the flowing gas takes away heat; and (3) it causes changes in solids inventory and the gas and solids residence times, both depending on the gas velocity.

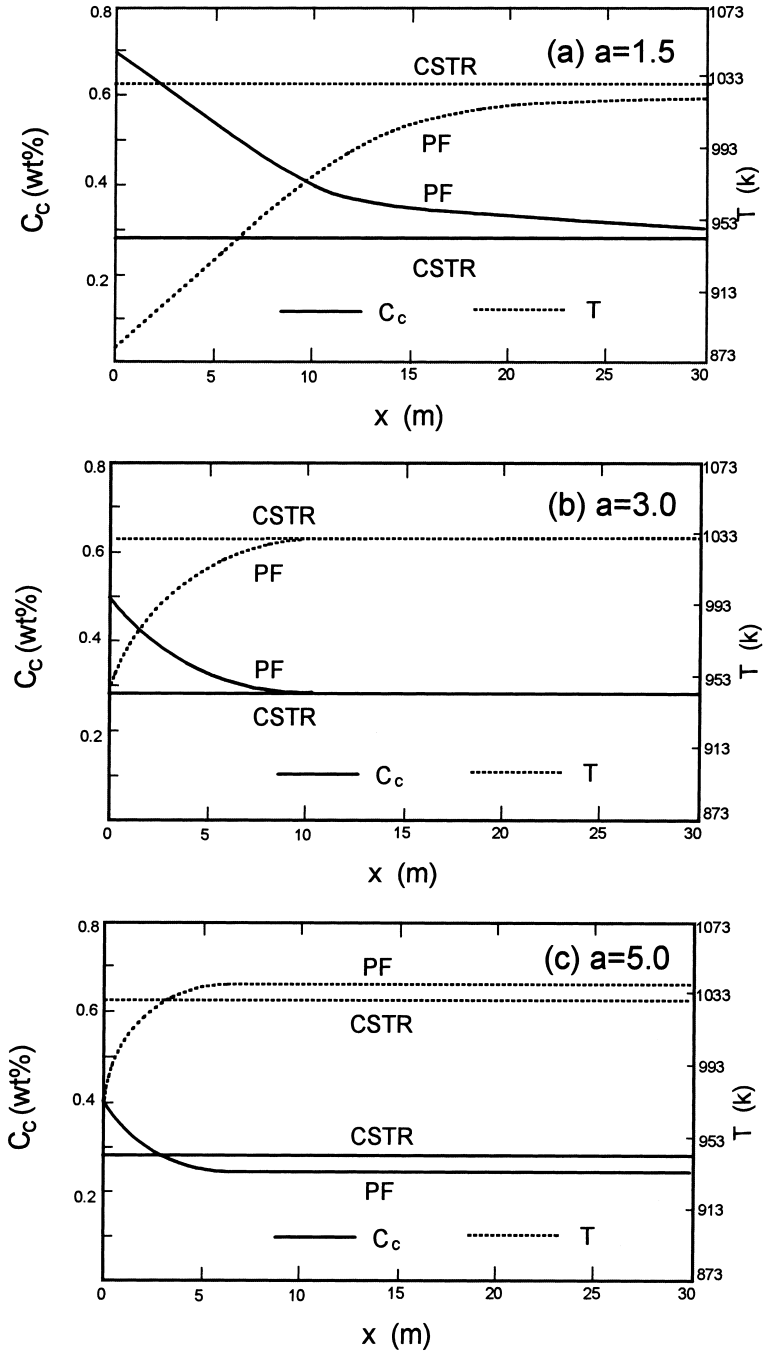

Fig. 6. Axial profiles of C_C and T predicted by the PF model and the CSTR model for (a) a=1.5, (b) a=3.0 and (c) a=5.0.

Since the gas velocity at the riser entrance also changes with the temperature of the regenerated catalyst (i.e. the temperature at the exit), some other factors such as the solids circulation rate will also influence the regeneration through the resulting variation in gas velocity. For correct comparison, the gas velocity presented in this paper is the velocity under standard conditions. This standard gas velocity is then changed to its appropriate value by applying ideal gas law in the simulations.

Fig. 7 shows the carbon content, oxygen concentration and temperature at the riser exit as a function of gas velocity. It is found that for both the PF and the CSTR modes, low gas velocity often denotes a high value of $C_{C,out}$ due to the insufficient oxygen to completely combust the carbon. Although increasing gas velocity would lower the solids inventory and shorten the solids residence time, both negative effects on the regeneration performance, the increased oxygen supply due to increased gas velocity over-compensates these negative effects and further improves the regeneration, which leads to decreased $C_{C,out}$ (see also Fig. 4). However, when the gas velocity is too high, the entrance temperature would drop to a significantly low value such

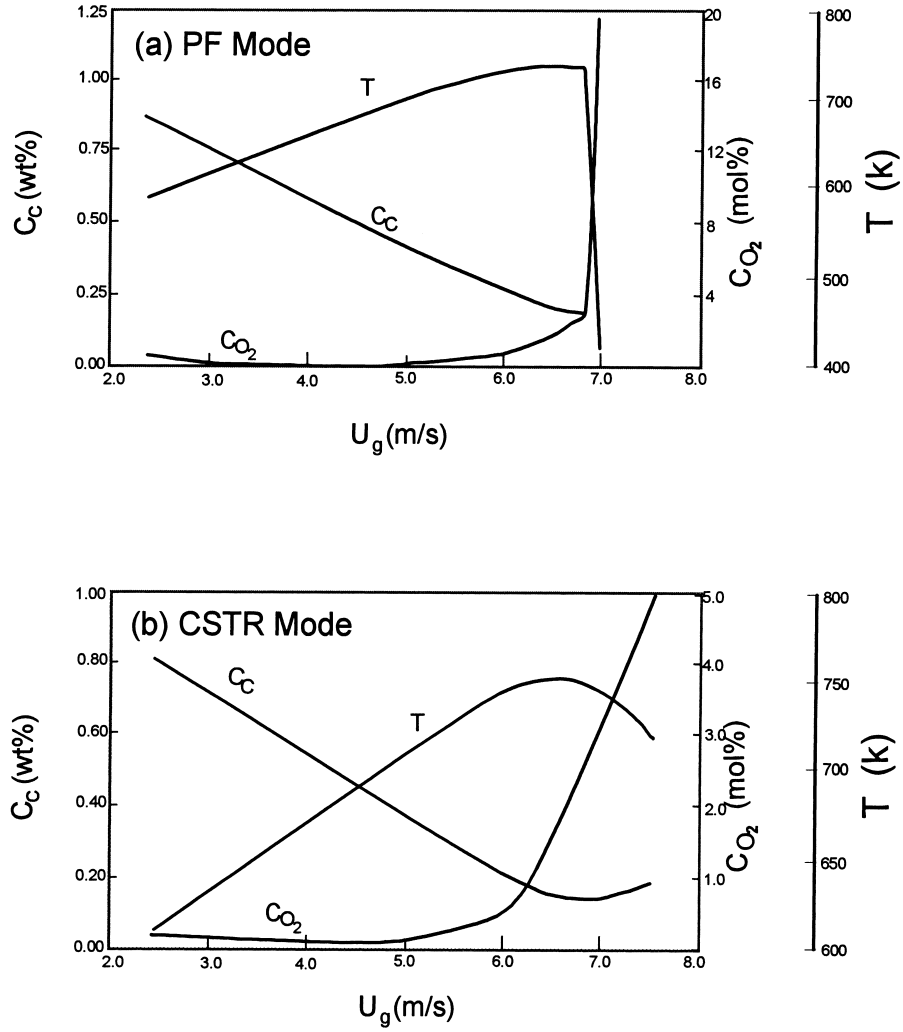

Fig. 7. Influence of gas velocity on C_C, C_{O_2}, and T at the riser exit (G_{ss}=50 kg/m^2 s, C_{Cs}=1.25%, α=0.087, T_a=40°C, T_s=490°C, p=253.25 Pa and a=3.0).

that the regenerator can no longer be operational (at ~6.8 m/s for the case shown in Fig. 7). This is referred to as quenching. As a compromise, the preferable oxygen concentration at the riser exit should be in the range of 2–4 mol% in order to maintain a good operation and to obtain lower $C_{C,out}$. Fig. 7 also shows that the influence of the superficial velocity on riser regeneration is similar for both the PF and the CSTR modes.

3.4. Influence of spent catalyst circulation rate, G_{ss}

The influence of spent catalyst circulation rate, G_{ss}, on the regeneration performance is shown in Fig. 8 for a given gas velocity (U_{g0}=5 m/s) and a constant catalyst recirculation ratio (a=3). In general, increasing the spent catalyst feed rate without correspondingly increasing the air flowrate would increase the carbon content on the regenerated catalyst due to the relatively reduced oxygen supply. Besides this, increasing G_{ss} would, on one hand, benefit the regeneration due to the corresponding increase in the amount of carbon, which increases the riser temperature given the increased reaction heat produced. On the other hand, the temperature in the entrance region of the regenerator will be lowered with increasing G_{ss} due to the decreased riser exit (and, therefore, recirculated) catalyst temperature. This in turn slows down the regeneration reactions. Competition between the above factors will finally determine how the regeneration performance will vary with G_{ss}. For the conditions indicated in Fig. 8, when G_{ss} is increased from 30 to 40 kg/m^{2}s (curves A and B), the heat produced due to the accelerated reactions predominates over the decrease in exit temperature, resulting in a slight increase in temperature. However, the limited oxygen supplied by the fixed gas flowrate cannot meet the demand for reaction with more carbon and hydrogen so that the carbon content at the riser exit increases with increasing G_{ss}. Further increasing G_{ss} to 50 kg/m^{2}s (curve C), a large drop in temperature is seen, which greatly slows down the regeneration. As a result, carbon and hydrogen contents at the riser exit increase significantly. A slight increase in oxygen concentration is also observed due to the extremely low reactivity.

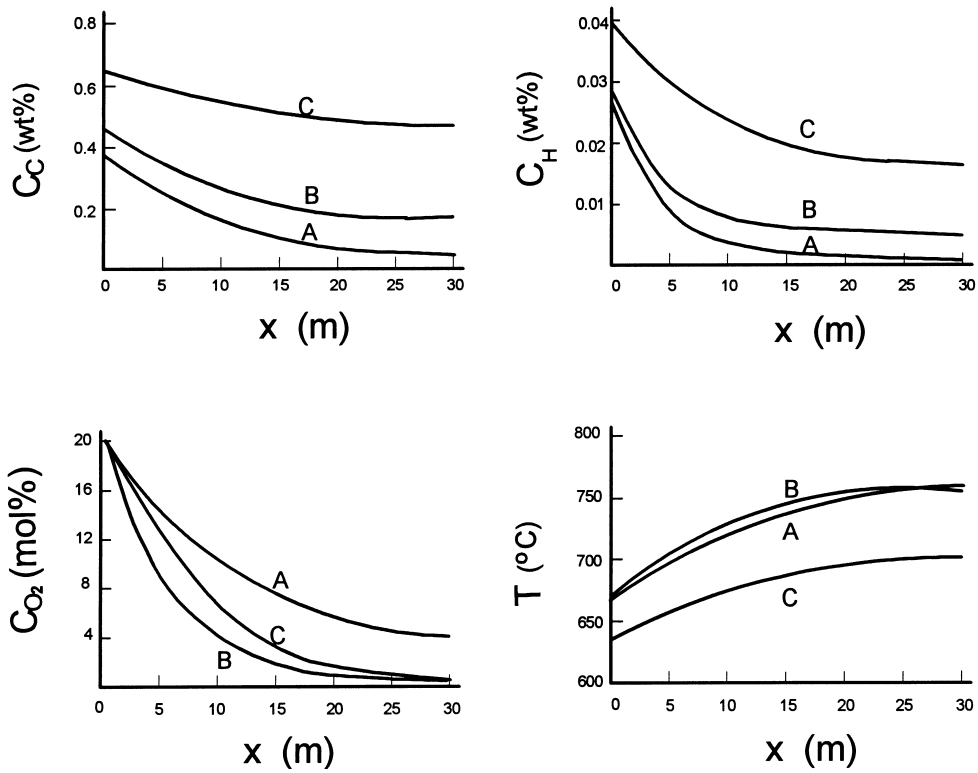

Fig. 8. Influence of circulation rate of spent catalyst for G_{ss}=30 kg/m^2 s (curve A), G_{ss}=40 kg/m^2 s (curve B), G_{ss}=50 kg/m^2 s (curve C) (U_{g0}=5 m/s, a=3.0, C_{Cs}=1.25%, α=0.087, T_a=40°C, T_s=490°C and p=253.25 Pa).

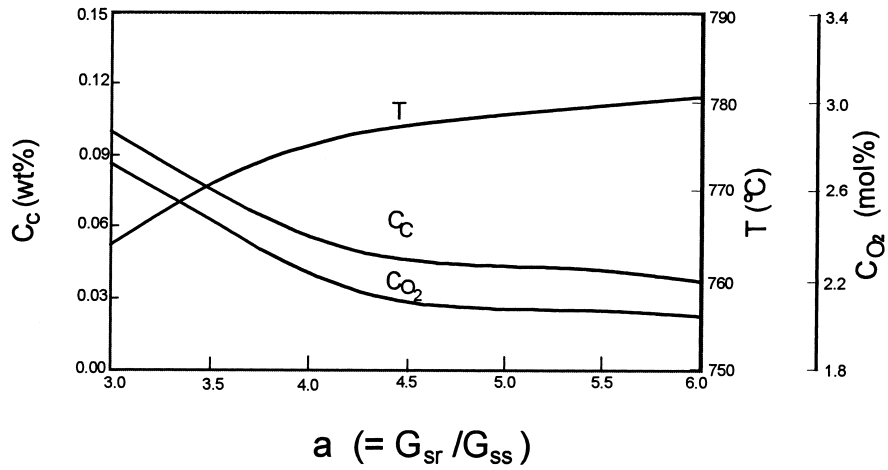

Fig. 9. Influence of the ratio of recycled to spent catalyst flowrates (U_{g0}=6 m/s, G_{ss}=40 kg/m^2 s, C_{Cs}=1.25%, α=0.087, T_a=40°C, T_s=490°C and p=253.25 Pa).

3.5. Influence of the recirculation ratio, a

The influence of the recycled (regenerated) to spent catalyst flowrate ratio, defined by $a = G_{sr}/G_{ss}$, on the regenerator performance has been shown in Fig. 9. One can clearly see that the carbon content on the catalyst at the riser exit always decreases with increasing a. This is mainly benefited from the increase in the temperature as a is increased. Simulation indicates that the influence of a becomes insignificant when a is relatively large since in this case the temperature of the entrance approaches that of the exit, as shown in Fig. 6. Note that the increase in a reduces the combustion intensity of the regenerator, and is sometimes limited by the unit capacity. Therefore, an optimal value of a is recommended in practical operation.

3.6. Influence of carbon content on the spent catalyst, C_{Cs}

Simulation results for C_{Cs}=0.8 wt.% (curve A) and 1.2 wt.% (curve B) are compared in Fig. 10. Clearly, lower

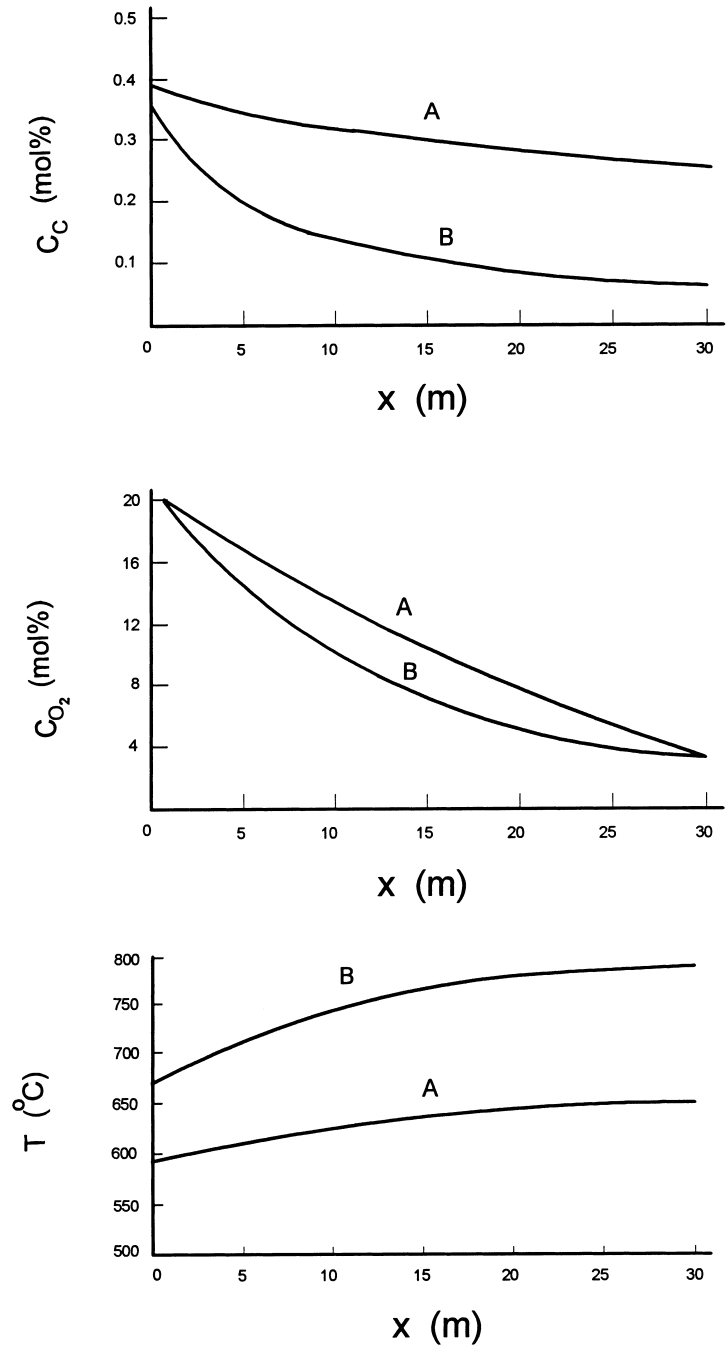

Fig. 10. Axial profiles of carbon content, oxygen concentration and temperature for C_{Cs}=0.8 wt.% (curve A) and C_{Cs}=1.2 wt.% (curve B) (U_{g0}=6 m/s, G_{ss}=40 kg/m^2 s, a=3.0, $C_{O_2,out}$=3.0%, α=0.087, T_a=40°C, T_s=490°C and p=253.25 Pa).

carbon content on catalysts is observed as C_{Cs} is increased. This is because higher carbon content on the spent catalyst increases the carbon concentration in the riser entrance and thus stimulates the regeneration reactions, eventually giving rise in temperature which in turn accelerates the reactions. However, it should be pointed out that C_{Cs} cannot be increased indefinitely since the produced heat will raise the riser temperature to such an extent that the catalyst would be severely deactivated due to steaming. This can be a severe limitation to riser regeneration. To overcome this, novel riser regenerator technologies such as multi-air supplies and a two-staged riser [23,24] have been proposed to meet the special demands for heavy oil processing.

3.7. Influence of air and spent catalyst temperatures

As shown in Figs. 11 and 12, there is a minimum temperature below which the regeneration reactions will quench due to extremely low temperature. The magnitude

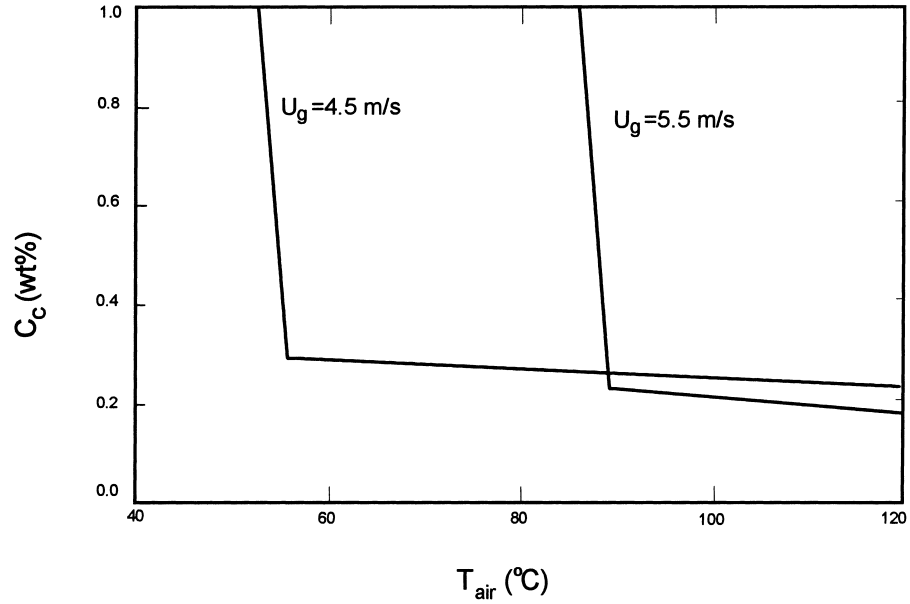

Fig. 11. Influence of air temperature (G_{ss}=40 kg/m^2 s, a=2.0, C_{Cs}=1.25%, α=0.087, T_s=490°C and p=253.25 Pa).

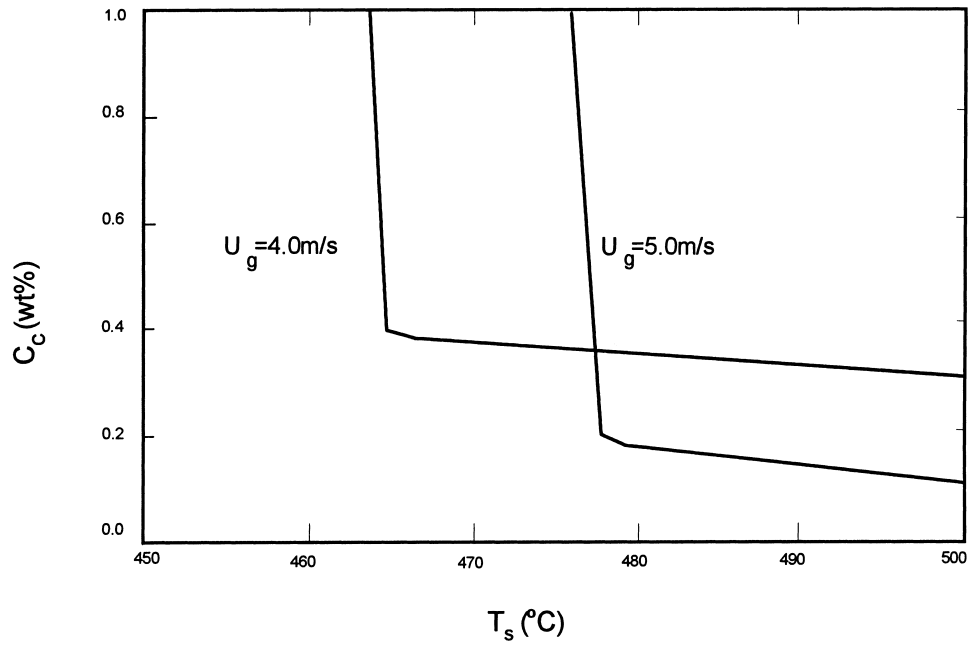

Fig. 12. Influence of spent catalyst temperature (G_{ss}=40 kg/m^2 s, a=3.0, C_{Cs}=1.25%, α=0.087, T_a=40°C and p=253.25 Pa).

of this minimum temperature depends on the operating conditions. Above this temperature, the carbon content at the riser exit decreases only slightly with increasing the temperature of the air and/or the spent catalyst.

4. Conclusions

A one-dimensional model is developed in this work to study the regeneration performance of a novel riser regenerator. The model incorporated comprehensive hydrodynamics in circulating fluidized bed risers and the kinetic characteristics of FCC catalyst regeneration. Initial simulations have been validated by the data obtained from an industrial unit. Axial profiles of temperature, oxygen concentration and coke content on catalyst particles are predicted for different operating conditions. Simulation results indicate that FCC catalyst regeneration is a very complex process and many factors (solids mixing pattern, gas velocity, catalyst circulation rate, the regenerated catalyst recycle ratio, air and spent catalyst temperatures, as well as carbon content on the spent catalyst) influence the

regeneration performance. Generally speaking, temperature plays a very important role in regeneration. It is preferable to maintain a temperature that gives high enough reaction rates and thus lower carbon content on regenerated catalysts. Caution should be made not to operate the regenerator at such a low temperature that it begins to quench the reaction or at such a high temperature that the FCC catalyst becomes deactivated due to steaming generated from hydrogen combustion.

Acknowledgements

This work is funded by both SINOPEC and Chinese National Nature Science Foundation. The assistance of Mr. Q.-Y. Yang in obtaining the data of industrial regenerator is acknowledged. The authors are also grateful to Prof. G.-H. Yang, president of University of Petroleum (China), for providing the detailed regeneration kinetics.

Appendix

Nomenclature

a ratio of recycled to spent catalyst flowrates ($=G_{sr}/G_{ss}$)
C_C carbon content on catalyst (wt.%)
C_{Cs} carbon content on spent catalyst (wt.%)
C_D drag coefficient
C_{DS} standard drag coefficient
C_H hydrogen content on catalyst (wt.%)
C_{O_2} oxygen concentration (kmol/m^3)
c_{pg} specific heat capacity of gas (kJ/kg °C)
c_{pc} specific heat capacity of catalyst (kJ/kg °C)
D riser diameter (m)
d_p mean diameter of catalyst particles (m)
F_D drag force between gas and particles (N)
F_g friction force between gas and wall (N)
F_p friction force between solids and wall (N)
f_g friction coefficient between gas and wall
f_p friction coefficient between solids and wall
G_g gas flowrate (kg/m^2 s)
G_s total catalyst flowrate ($=G_{ss}+G_{sr}$, based on the cross-sectional area of riser) (kg/m^2 s)
G_{sr} recycled catalyst flowrate (based on the cross-sectional area of riser) (kg/m^2 s)
G_{ss} spent catalyst flowrate (based on the cross-sectional area of riser) (kg/m^2 s)
k_C carbon combustion reaction constant (1/kPa min)
k_H hydrogen combustion reaction constant (1/kPa min)
p pressure (kPa)
p_{O_2} partial pressure of oxygen (kPa)
R ideal gas constant (R=8.314 kJ/kmol K)
Re Reynolds number defined by $\mathrm{Re} = d_p U_g \rho_g/\mu$ or $\mathrm{Re} = DU_g\rho_g/\mu$
$\mathrm{Re_r}$ Reynolds number defined by $\mathrm{Re_r} = d_p(\bar{V}_g - \bar{V}_p)\rho_g/\mu$
$\mathrm{Re_t}$ Reynolds number defined by $\mathrm{Re_t} = d_p v_T \rho_g/\mu$
r_C carbon combustion rate (kg/kg-cat s)
r_H hydrogen combustion rate (kg/kg-cat s)
T temperature (°C)
T_a air entrance temperature (°C)
T_g temperature of regenerated catalyst at the entrance (°C)
T'_g temperature of regenerated catalyst at the exit (°C)
T_s temperature of spent catalyst (°C)
t time (s)
U_g superficial gas velocity (m/s)
$\bar{V}_g$ cross-sectionally averaged actual gas velocity (m/s)
$\bar{V}_p$ cross-sectionally averaged actual solids velocity (m/s)
v_T terminal velocity of a single particle (m/s)
x axial coordinate (m)
x_{O_2} mole fraction of oxygen

Greek letters

α mass ratio of hydrogen to carbon in coke
β mole ratio of CO_2 to CO in the flue gas
ΔH_C entropy due to carbon combustion (kJ/kg)
ΔH_H entropy due to hydrogen combustion (kJ/kg)
$\bar{\epsilon}$ cross-section average voidage
ϵ_a cross-section average voidage at riser entrance
$\bar{\epsilon}_v$ average voidage over the whole riser
ρ_g gas density (kg/m^3)
ρ_p particle density (kg/m^3)
μ gas viscosity (Pa s)

Subscript

0 standard condition (273 K and 101.3 kPa)

out exit

References

[1] A.A. Avidan, M. Edwards, H. Owen, Innovative improvements highlight FCC's past and future, Oil and Gas J. 88(2) (1990) 33–58.
[2] A.M. Squires, M. Kwauk, A.A. Avidan, Science 230 (1985) 1329–1337.
[3] R.J. Gartside, QC-a new reaction system, in: J.R. Grace, L.W. Schemilt, M.A. Bergougnou (Eds.), Fluidization VI, Engineering Foundation, New York, 1989, pp. 25–32.
[4] Z. Wang, D. Bai, Y. Jin, Hydrodynamics of a concurrent downflow circulating fluidized bed (CDCFB), Powder Technol. 70 (1992) 271–275.
[5] J.-X. Zhu, Z.-Q. Yu, Y. Jin, J.R. Grace, A. Issangya, Cocurrent downflow circulating fluidized bed (downer) reactors – a state of the art review, Can. J. Chem. Eng. 73 (1995) 662–677.

[6] T. Gauthier, The R2R IFP-Total Process for FCC, Presentation at the Conference on Chemical Reactor Engineering for Sustainable Processes and Products, Banff, Canada, June 1997.
[7] J.R. Grace, High-velocity fluidized bed reactors, Chem. Eng. Sci. 45 (1990) 1953–1966.
[8] J.R. Grace, G. Sun, Influence of particle size distribution on the performance of fluidized bed reactors, Can. J. Chem. Eng. 69 (1991) 1126–1134.
[9] A.A. Avidan, R. Shinnar, Development of catalyst cracking technology: a lesson in chemical reactor design, Ind. Eng. Chem. Res. 29 (1990) 931–942.
[10] A.M. Squires, The story of fluid catalytic cracking: the first circulating fluidized bed, in: P. Basu (Ed.), Circulating Fluidized Bed Technology, Pergamon Press, New York, 1986, pp. 1–19.
[11] S. Dutta, B.R. Christian, M.F. Raterman, Circulating fluid bed reactor model developed for FCC/ART regenerator, in: J.R. Grace, L.W. Schemilt, M.A. Bergougnou (Eds.), Fluidization VI, Engineering Foundation, New York, 1989, pp. 9–16.
[12] D. Bai, Y. Jin, Z.-Q. Yu, One-dimensional steady-state gas–solids flow model in fast fluidized bed, J. Chem. Eng. Chinese Univ. 4(2) (1990) 112–121.
[13] D. Bai, Y. Jin, Z.-Q. Yu, Acceleration of particles and momentum exchange between gas and solids in fast fluidized beds, in: M. Kwauk, M. Hasatani (Eds.), Fluidization'91 – Science and Technology, Science Press, Beijing, 1991, pp. 46–55.
[14] L. Schiller, Z. Naumann, Ver dtsch, Ing. 77 (1933) 318–325.
[15] J. Martin, E. Michaelides, in: Proceedings of the Third Multiphase Flow and Heat Transfer Symposium Workshop, Miami Beach, 1983, pp. 353–360.
[16] Y.-Y. Zheng, S.-L. Gao, Petroleum Refinery (in Chinese) 5 (1986) 45–49.
[17] W.-J. Mo, S.-X. Lin, G.-H. Yang, Petroleum J. (Petroleum Processing) 2(2) (1986) 13–19.
[18] W.-J. Mo, S.-X. Lin, G.-H. Yang, Petroleum J. (Petroleum Processing) 2(3) (1986) 11–18.
[19] C.-L. Peng, G. Wang, Petroleum J. (Petroleum Processing) 3(1) (1987) 17–25.
[20] M. Kwauk, N.-D. Wang, Y. Li, B.-Y. Chen, Z.-Y. Shen, Fast fluidization at ICM, in: P. Basu (Ed.), Circulating Fluidized Bed Technology, Pergamon Press, New York, 1986, pp. 33–62.
[21] D. Bai, N. Gan, Y. Jin, Z. Yu, Riser regeneration of FCC catalyst, Petroleum Refinery 19 (1991) 20–27.
[22] D. Bai, Y. Jin, Z. Yu, Flow regimes in circulating fluidized beds, Chem. Eng. Technol. 16 (1993) 307–313.
[23] Y. Jin, Z.-Q. Yu, D. Bai, F. Wei, Chinese Patent, No. 932199720, 1993.
[24] D. Bai, J. Zhu, Y. Jin, Z.-Q. Yu, Novel designs and simulation of FCC riser regeneration, I & EC Res. 36 (1997) 4543–4548.